Understanding Parameters Influencing Tire Modeling

Nicholas D. Smith
Colorado State University, 2004 Formula SAE Platform

ABSTRACT

The purpose of this document is to describe important tire characteristics and their effect on vehicle performance. Characteristics considered are those that the Formula SAE judges have deemed important for discussion on tires at competition and include coefficient of friction, slip angle, slip ratio, camber angle, cornering stiffness, camber stiffness, self-aligning torque, normal load sensitivity, load transfer sensitivity and pneumatic trail. Every effort has been made to list sample values to give the reader a general idea for common values of the considered characteristics. Values relating to a typical FSAE vehicle are also listed for available data.

INTRODUCTION

The importance of the tire's contribution to a racing vehicle cannot be overstated. Tires are required to produce the forces necessary to control the vehicle. Given that the tire is the only means of contact between the road and the vehicle, they are at the heart of vehicle handling and performance.

Insight into the discussed parameters will help the FSAE student in various ways. Knowledge of these characteristics and their effects on racecar performance can give the engineer insight into performance optimization. A firm grasp on what influences a tire's behavior and what these characteristics mean in terms of vehicle dynamics terminology will better prepare the student to score higher during design judging at competition.

This document only covers one small piece of a very complex assembly. However, the tire itself is also extremely complex. The information contained within should allow the reader to grasp the vehicle dynamics terminology considering tires with much less effort than if the tire had to be researched independently.

TIRE BACKROUND

While the wheel may have been one of man's first inventions, the rubber tire is definitely not one of the simplest components to analyze. The rubber tire is a complex composite consisting mainly of vulcanized rubber, which more specifically is an elastomer with a high number of sulfur cross-links between the polymer chains. The composite also contains carbon black, oil extenders and layered reinforcing strands or fabrics called plies. These strands are normally made of Nylon, Terylene, Rayon or steel cords and are oriented in various configurations (Ref 1). While much attention is paid to the rubber itself, the reinforcing cords also deserve attention. These cords have a higher modulus of elasticity and less creep and therefore carry the load while the rubber skin serves to seal the air. An in depth study of tire construction would show that cord orientation (radial or bias ply) can have a significant effect on tire characteristics. Racing tires are set up in a bias ply configuration, providing strength in the three planes simultaneously (Ref 2).

Rubber tires have been present for quite some time and have seen many improvements such as the use of Vulcanization by Goodyear in 1839 and the addition of carbon black by Pirelli in 1907 (Ref 1). With these improvements, the rubber tire has produced superior control and durability when compared with other substitutes that have been attempted over the years.

NOTATION

It is important first to review a tire in its most general orientation and consider the forces acting on a tire. The SAE tire axis terminology is shown in Figure 1. The axis system is not the same as the axis system on the 2004 Platform racecar. The SAE system (SAE J670e) denotes the X being forward, Y to the right and Z downward. The 2004 FSAE Platform racecar uses X forward, Y left, and Z upward.

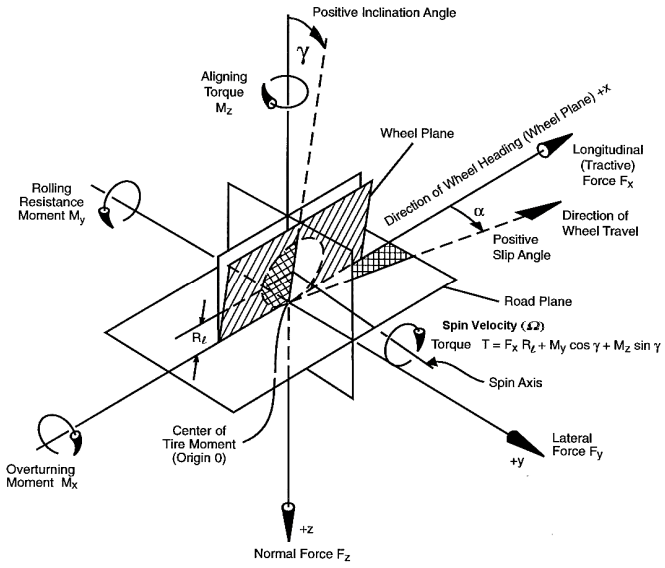

Figure 1 - SAE Axes Terminology (from Ref 4)

There are several forces, moments and angles that prove to be very important in tire behavior. All these forces can be seen as the forces and moments acting on the tire from the road. First, there are two main angles to consider, the camber angle and the slip angle. The camber angle is the inclination angle from its vertical position while the slip angle is the difference in wheel heading and direction. These two angles are associated with the lateral force. Forces include the longitudinal force in the X direction, the lateral force in the Y direction and the normal force in the Z direction. Longitudinal force (F_X) is the result of the tire exerting force on the road and becomes negative during braking. The lateral force (F_Y) is the resultant of the forces produced by a non-zero camber angle and by a non-zero slip angle during cornering. Normal force (F_Z) can also be viewed as the negative of the upward vertical force. Moments include the overturning moment, the rolling resistance moment, the wheel torque and the aligning moment. The overturning moment (M_X) is caused by a lateral shift of the vertical load during cornering. Rolling resistance (M_Y) is created by various factors that lead to a loss of energy. The aligning moment (M_Z), also known as the self-aligning torque, produces a restoring moment on the tire to realign the direction of travel with the direction of heading when the slip angle is non-zero. It should also be noted that there is also a moment produced by the axle on the wheel. As a final point, it may be noted that when the camber angle is zero, the wheel torque (T_{in}), points in the negative Y direction.

A list of acronyms and abbreviations is included at the end of this paper for reference.

PRINCIPLE TIRE MODELS

As stated earlier, tires are a complex composite comprising many layers of materials (see Figure 2 (Ref 3)). A tire is very anisotropic. It is for this reason that tire behavior is not derived from the material properties and structure of a tire. Simplifications are therefore made in order to create empirical models for a tire. The three foremost models used to understand tire forces, deflection and footprint behavior through the corning process are the elastic foundation model, the string model and the beam model (Ref 1). While none of these models truly addresses the complexity of a physical tire, realistic results can be obtained when empirical stiffness values are used.

Figure 2 - Section of the Common Tire (Ref 3)

Each small element in the elastic foundation model is considered to act independently of the other elements (see Figure 3). The aspect that each element acts as a simple spring, independent of the other elements, makes this model the simplest of the three. It is interesting to note that the force found under the curve of the lateral force distribution is equal to the lateral force measured at the axle (Ref 4). This supports the belief that although this model may be the simplest, it can be very useful in predicting and illustrating various tire behaviors, as is done by Dixon (Ref 1). The elastic foundation model also allows for discontinuity in the distribution of displacement and in the slope of the centerline. Conversely, in the string model, lateral displacement is also resisted by a tension between the elements. It also allows for discontinuity in slope, however, discontinuity in displacement is not allowed. Similar to the string model is the beam model, where each element has an effect on the surrounding elements. In the beam model, each element creates bending moments on the elements next to it. This allows no discontinuity in slope or displacement. The beam model has been found to be superior for radial ply or for belted bias ply tires (Ref 1). Often times a combination of these models will be combined to gain a better model (as was done by the U.S. Army Engineer Research and Development Center in their testing (Ref 5)).

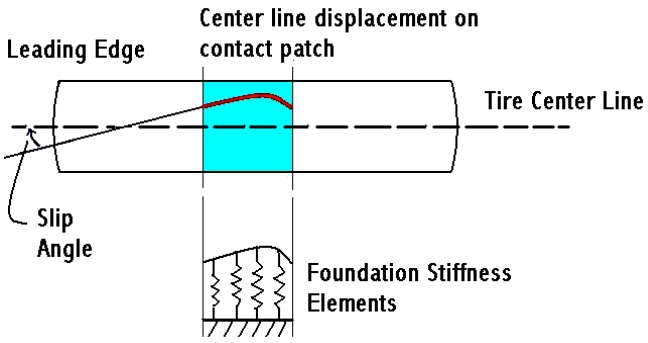

Figure 3 - Top View of Tire's Lateral Center Line Displacement During Cornering and Corresponding Foundation Stiffness Model (Ref 1)

COEFFICIENT OF FRICTION

The coefficient of friction is defined as a unitless ratio of friction force to normal force. It is generally considered true that the resulting friction force is not proportional to the surface area of contact. However, this is far from the truth when a rubber tire is considered. This dissimilar behavior is due to the viscoelastic nature of rubber. Thus, as force is applied, deformation occurs both elastically and plastically in a non-linear fashion due to the mechanical behavior of polymer chains (Ref 6). Viscoelasticity also explains why the coefficient of friction of a tire is load dependent. As a tire is loaded, the surface area grows larger increasing the total friction force but lowering the coefficient of friction (Ref 1). Since a tire does not follow Newton's laws of friction, a coefficient of friction above unity can be obtained. For example, given a 500 lb normal load on a tire, it would not be uncommon for a tire to produce 800 lb of force giving a coefficient of friction of 1.6. Under ideal conditions, this would make the vehicle capable of pulling 1.6 g's (Ref 2). However, ideal conditions are rarely achieved because the coefficient of friction depends on many transients.

The coefficient of friction can depend on many unknown variables such as atmospheric dust, humidity, temperature, vibration and the extent of contamination (Ref 7). It may also depend on the angularity of the road surface, speed, and even skid duration. As a tire skids further, the temperature rises above the optimal value, and the coefficient of friction begins to drop. Similarly, as the speed increases, temperature increases and the coefficient of friction again begins to decrease after reaching an optimum value (plotting coefficient of friction vs. velocity yields a curve that closely resembles a normal distribution). A final component that should not be overlooked is the molecular bonding that occurs which lends to total friction. While this adhesion between the road and tire does not require energy to create the bond, energy is dissipated when the bonds are broken. This becomes important in dry conditions. Conversely, the tire elastically conforming to the road becomes more important in wet conditions. (Ref 1)

Finally, some effects of the coefficient of friction changing with speed should be discussed. When slip angle become large, the rear of the footprint begins to slide and thus has a lower coefficient of friction. Therefore, the cornering force will top out at a modest slip angle and then begin to decline. This phenomenon is more dramatic in a locked wheel when braking. Since the wheel is locked, the local temperature rise is greater and the relative sliding speed is greater than for a rotating wheel. In either case, the decreased coefficient of friction contributes to a negative self aligning moment. (Ref 1)

For a more in-depth understanding of friction interactions with rubber tires, one can reference items 1 and 2 under Recommended Reading.

SLIP ANGLE

If the direction of travel differs from the wheel heading (if the wheel's angular displacement is different from the path the tire is following), the slip angle (α) produces a component of lateral force (F_Y). This lateral force will act through a point behind the center of the wheel in a direction such that it attempts to re-align the tire. It should be noted that the slip angle is not the same as the steering angle.

As can be seen from the elastic foundation model, there is a final fiction limited value of the lateral force due to slip angle that is reached (Ref 1).

$$c \cdot d \le \frac{\mu \cdot F_V}{l}$$

Equation 1

This equation, with c being the foundation stiffness, d being the tire centerline displacement and l being the tire footprint length, must be satisfied for no sliding. It then follows that the lateral force is roughly proportional to the slip angle. This then gives the maximum non-slide force.

$$F_Y = \frac{1}{2} \cdot c \cdot l^2 \cdot \alpha$$

Equation 2

$$\frac{1}{2} \cdot c \cdot d_m \cdot l = \frac{1}{2} \cdot c \cdot l \cdot \left(\frac{\mu \cdot F_V}{c \cdot l} \right) = \frac{1}{2} \cdot \mu \cdot F_V$$

Equation 3

Therefore, the lateral force is proportional to the slip angle up to half the maximum total friction limit (Ref 1). This can be seen in Figure 4, which graphs lateral force against slip angle for some example values that were chosen to be similar to a typical FSAE tire. These values are a 200 lbf (890 N) normal force, a coefficient of friction of 1.5, a foundation stiffness of 725 psi (5 MPa) and a contact patch length of 8.5 in (216 mm). The actual calculations can be seen in the appendix.

As can be seen in Figure 4, the upper limit is reached very quickly with the maximum force occurring at 90° when the wheel is fully sideways. Generally, a racing tire will achieve maximum lateral force at slip angles in the range of 3°-7° (Ref 4). In the figure below, the force at 3° is 95% of maximum. At high slip angles, the rear of the print actually slides laterally along the surface of the road, which contributes to less capacity for lateral force and reduces the stabilizing self-aligning torque (Ref 4).

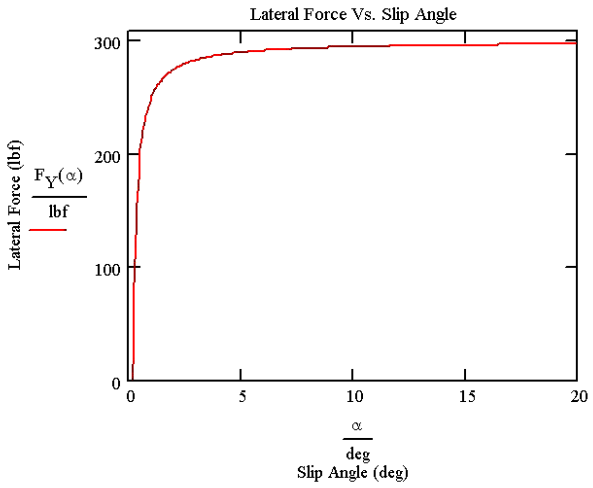

Figure 4 - Lateral Force vs. Slip Angle

It may be important to realize that when not completely sliding, the lateral force is not dependent on the coefficient of friction, although this provides the upper limit; instead, it depends on the foundation stiffness. An alternate way to look at this is to say that the lateral force is not dependent on coefficient of friction until the tire has "broken away", indicating a large slip angle (Ref 4). It is also sometimes convenient to define the lateral force due to slip angle in terms of other coefficients as seen in equations 4 and 5.

$$F_Y = F_\alpha = C_\alpha \cdot \alpha = C_S \cdot F_V \alpha$$ **Equation 4**

$$C_\alpha = C_S \cdot F_V$$ **Equation 5**

C_S is the cornering stiffness coefficient and C_α is the cornering stiffness. Generally, typical values for the cornering stiffness coefficient are 0.12/deg for bias-ply tires and 0.16/deg for radial ply tires. (Ref 1)

CORNERING STIFFNESS

The cornering stiffness can also be defined on a per radian basis as shown in equation 6.

$$C_\alpha = \frac{1}{2} \cdot c \cdot l^2$$ **Equation 6**

Cornering stiffness can also be seen to be the initial slope of the lateral force curve. Typical values for cornering stiffness' are around 195 $^{lbf}/_{deg}$ (867 $^{N}/_{deg}$) (Ref 1). However, this value can be much higher. For example, an Indy Road tire and a Formula 1 tire may have a C_α of 833 $^{lbf}/_{deg}$ (3.7 $^{KN}/_{deg}$) at 1800 lbf (8 KN) normal load and 750 $^{lbf}/_{deg}$ (3.4 $^{KN}/_{deg}$) at 1000 lbf (4.5 KN) normal load respectively (Ref 4). A tire for formula SAE would have a C_α around 165 $^{lbf}/_{deg}$ (734 $^{N}/_{deg}$) for a 330 lbf (1.5 KN) tire load as can be seen in Figure 15 (also see Avon Tire Curves in the Appendix). Notice how the cornering stiffness is sensitive to the range of slip angle used to find the slope on the lateral force curve. This further emphasizes that one should use caution when using cornering stiffness values in calculations, or at least realize its potential inaccuracies. As an additional point, the cornering stiffness is normally 5-6 times greater than camber stiffness for traditional bias tires (Ref 4).

Since the central/drag force ratio (see Equation 7 and Figure 5) reduces with slip angle, higher cornering stiffness is desirable. The reason for this is that a given central force will be achieved at smaller slip angles and therefore results in lower tire drag force. The central/drag ratio is given as follows (Ref 1):

$$\frac{F_S}{F_D} = \frac{C_\alpha \cdot \alpha \cdot \cos(\alpha)}{\mu_R \cdot F_V + C_\alpha \cdot \alpha \cdot \sin(\alpha)}$$ **Equation 7**

In this formula, μ_R is the rolling resistance, F_D is the drag force in the direction of travel, and F_S is the force component perpendicular to travel. F_D and F_S make up the components of the resultant lateral force F_Y.

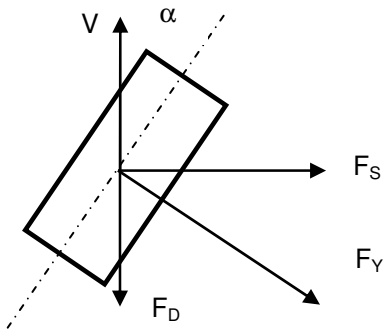

Figure 5 - Force Components for Undriven Tire (Ref 1)

The preceding formulas are valid primarily in the linear lateral force region. However, when more aggressive, larger camber angles are employed, as with a two-wheeled vehicle, the cornering stiffness may be reduced dramatically. When camber angle is included in the cornering stiffness, a new equation for cornering stiffness can be used.

$$C_\alpha = C_{\alpha 0} - k_{C\alpha\gamma}\cdot\gamma$$

Equation 8

Given that

$$\left(k_{C\alpha\gamma} = \frac{0.005}{\text{deg}}\right)$$

This equation is virtually linear up to about 60° (Ref 1). However, in a wide racing tire, large camber angles are rarely used as this would begin to lift one side of the tire off the ground. More on camber angle will be discussed in the following sections.

When trying to model the cornering coefficient accurately, it becomes evident that it is dependent on vertical load. The model that best fits analytical data is the exponential equation 9 as given below (Ref 1).

$$C_\alpha = C_{\alpha 1}\cdot\frac{F_V}{F_{V1}}\cdot e^{-K_{CSFV}\left(\frac{F_V}{F_{V1}}-1\right)}$$

Equation 9

The unitless value of K_{CSFV} is the sensitivity of C_S to F_V. The maximum cornering stiffness occurs when the vertical force is equal to the reference load over the sensitivity (F_{V1}/K_{CSFV}).

SLIP RATIO (% SLIP)

In contrast to slip angle, which is slip in the transverse plane, the slip ratio is the slip in the longitudinal plane. The slip ratio affects acceleration and breaking and therefore bears analogy to the slip angle in the sense that as slip angle is related to lateral force, slip ratio is related to longitudinal force and traction capacity. Generally speaking, the coefficient of friction will change with changing slip ratio. A plot of coefficient of friction vs. percent slip increases nearly linearly up to about 5% slip, peaks near 10% slip and then falls of in a nonlinear fashion (Ref 2).

The slip ratio can be defined empirically as a function of angular velocity of the driven wheels and angular velocity of the free rolling wheels. The slip ratio is defined in equation 10 (Ref 4).

$$SR = \frac{\Omega - \Omega_0}{\Omega_0} = \frac{\Omega\cdot R_e}{V\cdot\cos(\alpha)} - 1$$

Equation 10

The angular velocity of the driven wheel is Ω, the angular velocity of the free rolling wheel is Ω_0, R_e is the effective rolling radius and V is the velocity. Thus, for free rolling, SR = 0 while when locked under breaking SR = -1. For dynamic, real time testing, the effective radius cannot be measured; therefore, the loaded rolling radius is commonly used in its place. Slip percentage is simply the slip ratio expressed as a percentage (slip ratio multiplied by 100).

As stated earlier, longitudinal forces, tractive and breaking, are functions of the slip ratio. As the slip ratio increases, the longitudinal forces rise rapidly and then fall off after the maximum is reached in a range of 0.10 to 0.15 slip ratio (Ref 4). It can also be seen from Equation 10 that as the slip angle increases, the tractive or breaking force will decrease.

The definition of slip ratio used here is the equivalent of the SAE definition. Many other definitions and variations of slip ratio have been used and can be found in Ref 4.

CAMBER ANGLE

Camber angle is equal to inclination of the wheel from its vertical position. Or more precisely, camber is the inclination from a plane perpendicular to the ground. A positive camber angle is defined to be an outward lean such that the top of the tire leans outward from the vehicle centerline. A non-zero camber angle produces a camber force directed laterally toward the low axis side, producing another component of lateral force. Thus, a negative camber angle increases the lateral or cornering force of the tire. Generally, the lateral force produced from camber is a function primarily of tire stiffness, vertical force and camber angle. While there are other secondary forces present, such as friction effects and path curvature, these are small and can be neglected for most applications. Camber force can also be affected by the shape of the crown. A very round profile develops maximum lateral force with negative camber angles and a small slip angle while camber angles in the 0° - 4° negative range are better when a flatter crown is used (Ref 1). For wide street radial tires, camber force tends to fall off at camber angles above 5° (Ref 4).

With the combination of the preceding parameters, a new tire characteristic, camber stiffness, can be defined as the rate of change of camber force with change in camber angle. The equation for the lateral force component due to camber is seen in equation 11 (Ref 1).

$$F_Y = F_\gamma = C_\gamma\cdot\gamma = C_C\cdot F_V\cdot\gamma$$

Equation 11

F_Y is the lateral force, F_V is the normal force, γ is the camber angle, C_γ is the camber stiffness and C_C is defined to be the camber stiffness coefficient. A typical C_C value would be 0.018/deg for bias-ply tires and 0.008/deg for radial ply tires (Ref 1). While the camber force is usually less than the lateral force due to slip

angle (see Figure 6 and Figure 9), camber force can have a significant impact on vehicle handling, especially as suspension geometry may change.

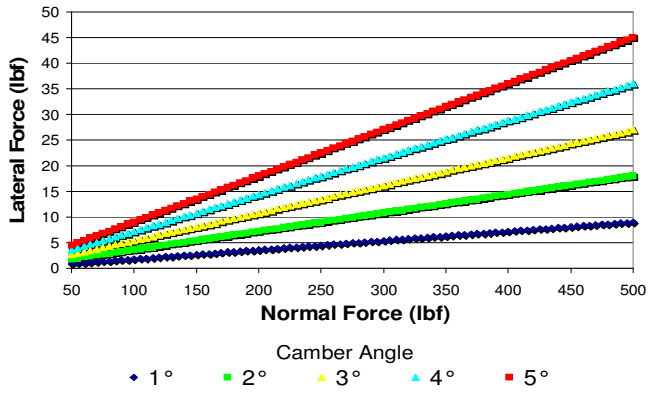

Figure 6 - Lateral vs. Normal Force for Varying Camber Angle

CAMBER STIFFNESS

The camber stiffness is the rate of change of camber force with camber angle ($\Delta F_Y/\Delta\gamma$) (Ref 4). A common value for camber stiffness is approximately 8 $^{lbf}/_{deg}$ (35.6 $^{N}/_{deg}$) which may be reduced significantly at speeds above 65 mph (104 $^{km}/_{hr}$) (Ref 1). The camber stiffness also decreases for large slip angles near the maximum lateral force. Generally, the camber stiffness is 5-6 times less than cornering stiffness for bias ply tires (Ref 4).

Camber force is due to lateral distortion in the contact patch of the tire. Thus, camber stiffness is often very small for radial tires due to the stiffness of the belt and the flexibility of the radial cords in the sidewall that prevent the lateral contact patch distortion (Ref 4).

TOTAL LATERAL FORCE

Now with the components of lateral force known, the total later force for small angles can be computed using superposition. Total lateral force is given in equations 12-14.

$$F_Y = F_\alpha + F_\gamma = C_\alpha \cdot \alpha + C_\gamma \cdot \gamma$$ **Equation 12**

$$F_Y = C_S \cdot F_V \alpha + C_C \cdot F_V \gamma$$ **Equation 13**

$$F_Y = F_V \left(C_S \cdot \alpha + C_C \cdot \gamma \right)$$ **Equation 14**

Path curvature is not included in these equations for lateral force. Path curvature is a small contribution and is often neglected for most cases (Ref 1). It may also be convenient to define a total lateral coefficient C_Y as shown in equations 15 and 16.

$$C_Y = C_S \cdot \alpha + C_C \cdot \gamma$$ **Equation 15**

$$F_Y = F_V \cdot C_Y$$ **Equation 16**

It can be seen that at maximum lateral force, camber force has only a small effect since the camber coefficient reduces for large slip angles.

COMBINED LATERAL AND LONGITUDINAL FORCES

It has been seen that the lateral force is highly correlated with the slip angle and the camber angle while the longitudinal force shows correlation with the slip ratio. Now it can be seen how these two forces affect the thrust or drag of the vehicle. Thrust or drag is defined in equation 17 (Ref 4).

$$TorD = F_X \cdot \cos(\alpha) - F_Y \cdot \sin(\alpha)$$ **Equation 17**

Formulation of an equation for rolling resistance (a drag force) can now also be seen in equation 18 (Ref 4):

$$F_R = \left[(SR + 1) \left(\frac{T_{in}}{R_l} \right) - F_X \right] \cdot \cos(\alpha) - F_Y \cdot \sin(\alpha)$$

Equation 18

In this equation, F_R is the rolling resistance, T_{in} is the input torque to the wheel, and R_l is again the loaded radius of the tire. Through inspection, it can be seen that the term $F_X\cos(\alpha)$ is the traction/braking component; $F_Y\sin(\alpha)$ is the induced drag due to lateral force, and F_R is the net rolling resistance (Ref 4).

A relationship for longitudinal force can also be formulated based on wheel input torque, wheel moments, camber angle and angular acceleration. This relationship is given in equation 19 (Ref 1).

$$-T_{in} + F_X R_l + M_Y \cos(\gamma) + M_Z \sin(\gamma) = I \dot{\Omega}$$

Equation 19

This equation can also be useful in calculating the longitudinal force. Note that when the camber angle is small, as well as the acceleration and rolling resistance, then the input torque is equal to the longitudinal force times the loaded radius (Ref 1).

SELF-ALIGNING TORQUE

Self-aligning torque, also known as self-aligning moment, is the resultant of the lateral force and the moment arm known as pneumatic trail, t. It is a restoring moment that attempts to return the wheels to a zero slip angle state (strait running). Essentially, the presence of the self-aligning torque exposes the fact that a tire likes to head

in the direction it is presently running. It may be important to note that the self-aligning torque may be influenced by a mechanical trail induced from suspension geometry. For example, more mechanical trail and therefore more self-aligning torque can be induced with the presence of caster and kingpin offset (Ref 4). Trail may also be affected by camber, which can induce a small destabilizing force (Ref 4). However, this is also small and often neglected. This discussion assumed no mechanical trail or trail effects due to camber.

Empirical equations for this torque have been derived from the foundation stiffness model and are as follows (Ref 1):

$$M_Z = F_Y \cdot t = \frac{F_Y \cdot l}{6} = \frac{c \cdot l^2 \cdot \tan(\alpha)}{12}$$ **Equation 20**

$$M_Z = \frac{\mu^2 \cdot F_V^2}{4 \cdot c \cdot l \cdot \tan(\alpha)} - \frac{\mu^3 \cdot F_V^3}{6 \cdot c^2 \cdot l^3 \cdot (\tan(\alpha))^2}$$ **Equation 21**

It should be noted that the above equations are for slip angles greater than the non-slide limit. The relationships defined by Equation 21 can be seen by graphing self-aligning torque over slip angle for various values of normal load as is done in Figure 7.

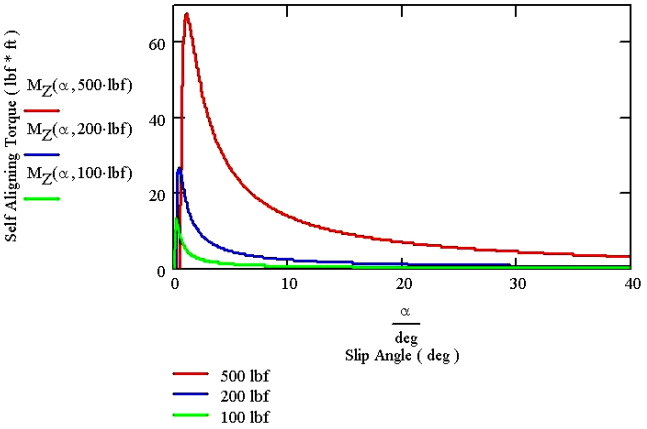

Figure 7 - Self-Aligning Torque vs. Slip Angle For Varying Normal Force

Many important relationships can be drawn from Figure 7. Potentially the most important is that as slip angle increases, thus increasing lateral force, the self-aligning torque decreases. This means that the driver's feel of the road through steering wheel torque is in essence removed as lateral force begins to reach its limit prior to sliding. However, this removal of feel gives the driver warning of front tire breakaway (Ref 2). Maximum warning of breakaway would occur when all the steering torque comes from the pneumatic trail. Mechanical trail substantially reduces the steering wheel torque (Ref 4).

The self-aligning torque can also be influenced by tire pressure. As the pressure is decreased, the contact patch lengthens and thus gives a longer moment arm, which in turn increases the aligning torque (Ref 4).

PNEUMATIC TRAIL

The pneumatic trail is essentially the moment arm through which the lateral force acts. As predicted by the foundation stiffness model, the lateral force acts behind the centerline of the tire. This is the result of the near-triangular contact patch distribution as shown earlier in Figure 3. The model predicts that this distance t is equal to the ratio of self-aligning moment to lateral force, or $^1/_6$ of the contact patch length as seen in equation 22.

$$t = \frac{M_Z}{F_Y} = \frac{1}{6}$$ **Equation 22**

While this model is reasonably accurate, larger values are commonly found when the slip angle is small. (Ref 1)

When using the foundation stiffness model to investigate further, Equation 23 is obtained for slip angles greater than the non-slide limit. This allows more relationships about the pneumatic trail to be distinguished. It can be seen that the pneumatic trail decreases once sliding beings and approaches zero when the slip angle is 90° (Ref 1).

$$t = \frac{3 \cdot \mu \cdot F_V \cdot c \cdot l^2 \cdot \tan(\alpha) - 2 \cdot \mu^2 \cdot F_V^2}{12 \cdot c^2 \cdot l^3 \cdot (\tan(\alpha))^2 - 6 \cdot \mu \cdot F_V \cdot c \cdot l \cdot \tan(\alpha)}$$ Equation 23

Part of the reason for the decrease in pneumatic trail, and the resulting reduction in self-aligning torque, is the increase in rear contact patch sliding. As the slip angle increases, more of the rear section of the contact patch beings to slide laterally. Since the footprint is sliding, it has less ability to stabilize the wheel. In this case, the aligning toque is reduced to near zero and may even reverse sign (Ref 4). The effects of the change in pneumatic trail and thus the location that the force acts on the contact patch can be seen in Figure 8, which shows how the force components change depending on steering. Figure 8 also shows a pressure distribution for the contact patch. Notice that for normal cornering the pneumatic trail is behind the centerline on the trailing edge side (TE). For severe cornering, the pneumatic trail is actually slightly ahead of the centerline toward the leading edge (LE).

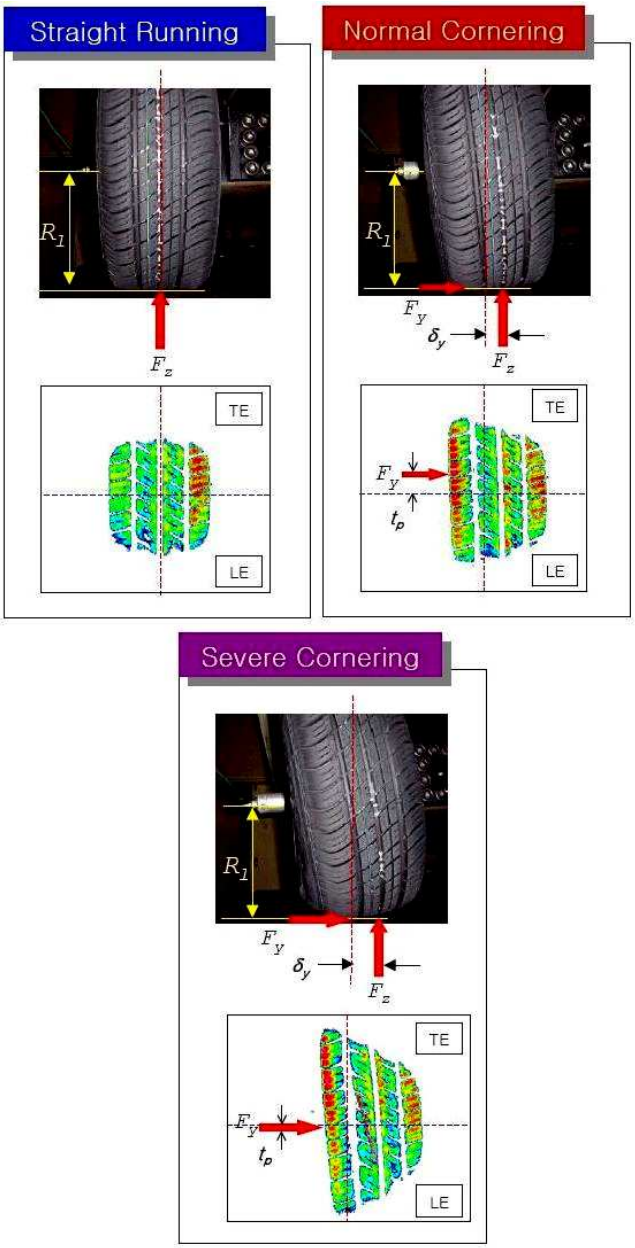

Figure 8 - Contact Patches for Various situations (Ref 3)

NORMAL LOAD SENSITIVITY

Normal load sensitivity is defined to be the rate of change of lateral force with the change in vertical force at a constant slip angle. The load sensitivity, C_{FV}, is defined in equation 24 (Ref 1):

$$C_{FV} = \left(\frac{\delta F_Y}{\delta F_V} \right)_{\alpha}$$

Equation 24

When plotting lateral force vs. normal load, it can be seen that there is not a proportionally greater increase in lateral force for an increase in vertical load, as can be seen in Figure 9. It should be noted that Figure 9 is based on empirical equations that are good for lower load ranges and actual data shows a nonlinear stabilization at higher loads and larger slip angles.

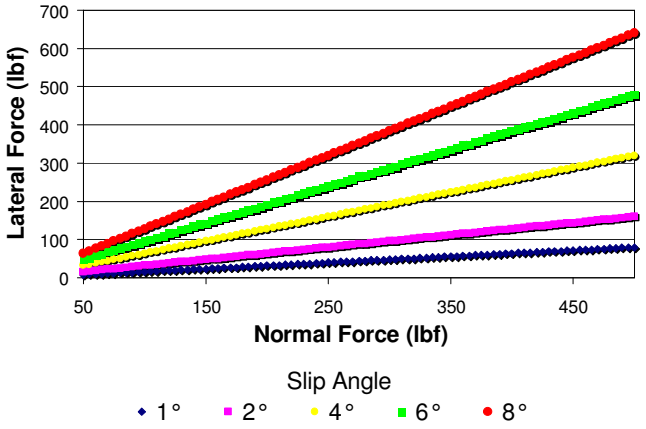

Figure 9 - Lateral vs. Normal Load for Varying Slip Angle

The load sensitivity tends to decrease as the normal load increases. This coefficient may run as high as 1.8 for current Grand Prix tires. Tire load sensitivity is more or less independent of speed. It can be increased by using a tire compound that is more "sticky" and by keeping temperatures in the desirable ranges. (Ref 4)

Using the 2005 CSU FSAE race car as an example, the normal load on a tire can change by as much as 116 lbf (516 N) for a 700 lbf (3.1 kN) car in a 1.5g turn as found by Adam Skaggs (Ref 8). Reference 4 can be consulted on calculating actual load transfer for a vehicle. An example of calculating normal load sensitivity for the Avon tire data can be found in the appendix.

LOAD TRANSFER SENSITIVITY

Load transfer can have a great impact on vehicle handling. Increasing the amount of uneven load distribution laterally from load transfer (such as having a non-central center of gravity) decreases the total lateral force that can be achieved. This effect is amplified at large lateral accelerations. The load transfer sensitivity between two wheels is defined mathematically in equation 25 (Ref 1).

$$C_{FT} = \left(\frac{\delta F_{Y2}}{\delta F_{VT}} \right)_{\alpha, F_{V2}}$$

Equation 25

F_{Y2} is the total side force for two wheels, and F_{VT} is the transferred vertical force. It is assumed that the total vertical load ($2F_V$) is constant as is the slip angle (α). This reduction in total lateral force is a second order effect since tire force varies nonlinearly with normal load (Ref 2). Even though load transfer always results in less

total force, load transfer may not be an undesirable phenomenon. If the load transfer is from the front to the rear wheels (longitudinal instead of lateral), the rear, heavier loaded pair of tires, now has an increased traction ability and can therefore accelerate more with less slip. This would be desirable if the car only had to accelerate forward. For a racecar that must corner, accelerate and break, it is more desirable to have the load transferred evenly over all the wheels.

The load transfer sensitivity and the normal load sensitivity are highly correlated. Since there are an enormous number of factors involved, it is difficult to list all relationships. However, it is generally the case that tires with a higher C_{FV} tend to let go or break away faster (Ref 4).

EXAMPLE CALCULATIONS

A few calculations are provided in order to give another set of example values and illustrate how one would use tire data. The example calculations can be seen in their entirety in the Appendix. Example calculations are based on data from the Avon tires, a tire that one of the CSU FSAE teams has been considering for use.

The calculations begin by assuming a few known values or values at a point of interest. These values include a slip angle of 1.3°, a camber angle of 1° (using data from Figure 13 and Figure 14), a 150 kg normal tire load and a coefficient of friction of 1.5. Since the slip angle is 1.3°, a point not shown in the figures, absolute values of data points from around this value were taken and used in a quadratic interpolation for higher accuracy. Lateral force and self-aligning torque were then calculated to be 187 lbf (831 N) and 23 ft*lbf (31.5 N*m) respectively. Using equation 22, the pneumatic trail and contact patch length were calculated to be 1.49 in (37.9 mm) and 8.95 in (227.3 mm) respectively. Equation 4 was then used for approximating the cornering stiffness, which was determined to be 143 $^{lbf}/_{deg}$ (639.5 $^{N}/_{deg}$). As a final consideration, the normal load sensitivity was found to be 0.582 using equation 24. The data used for this calculation was taken from Figure 14 in order to determine the lateral load at a vertical load of 150 kg and 250 kg at a 1.5° slip angle.

These values are hard to compare to other FSAE type tires due to lack of tire data. Therefore, no conclusion can be made about the Avon tires at this time. However, these values may be helpful in dynamic analysis concerning tires or wheels. It is also expected that as more data becomes available, these values will be helpful in choosing the best tire for the CSU FSAE racecar.

OTHER CONSIDERATIONS

TIRE PRESSURE

Tire pressure is one of the few parameters that the vehicle's operator can control. This may be part of the reason that it is one of the most common changes in setting up a racecar (Ref 4). Tire pressure can affect the tire's characteristics in a variety of ways. Being that the stiffness coefficients are essentially a measure of the elasticity of the tire, an increase in tire pressure will increase the stiffness of the tire. This will in turn increase the lateral force. If an inflation pressure 70% above the design value is used, a 20% gain in tire stiffness can be obtained. Increasing pressure above this will then decrease stiffness (Ref 1). Pressure variation from front to rear is often used to make minor adjustments in under/over steer balance of the vehicle (Ref 4). Tire drag is also decreased as pressure is increased.

In contrast to lowering pressure, raising the pressure will decrease the coefficient of friction. As mentioned earlier, lowering pressure will raise the coefficient of friction by reducing contact patch pressure and increasing the size of the contact patch. The increased contact patch also increases the self-aligning torque, as discussed earlier. Lowering the pressure also decreases the tire life and reduces the vehicles handling or feel (Ref 1).

Another consideration to deal with pressure is "ride". The pressure significantly affects the tire "ride", which is essentially a reflection of the tire's spring rate. It is often the case that a specific overall spring rate for an entire car is a design parameter (Ref 4). Therefore, the tire pressure may be constrained depending on the adjustability of the vehicles suspension system. Spring rate data for the Hoosier tire (the current FSAE tire) is given in the appendix.

There are tradeoffs in deciding what pressure to run at. Low tire pressures may benefit lap times due to better conformity; however, low pressures, or running with a slow leak, may lead to excessive tire temperatures. If pressure is too high, cornering power, acceleration and breaking may be adversely affected (Ref 2). As a result of the many factors, there is no one right pressure to run at. Individuals must experiment with their own setup to determine the optimal pressure for the application. As a final comment, it may also be noteworthy to point out that pressure and temperature relations may not be as expected depending on the moisture content of the compressed air used to fill the tire. Therefore, dry air is preferable (Ref 1).

TIRE TEMPERATURE

Tire temperature can change tire characteristics in a variety of ways. Specifically, temperature most heavily influences the forces produced by the tire but also affects the life of the tire.

The temperature affects the tire's stiffness, and therefore force, in at least two different ways. As the temperature changes, the modulus of elasticity will change thus changing the stiffness of the tire (Ref 4). Similarly, when tires run hot for extended periods, the pressure may also increase which again changes the tire stiffness. Dixon notes that the warmed-up pressure is typically 4.3psi (30kPa) higher than cold-set values (Ref1). The temperature will also influence the tire's force capability due to change in the coefficient of friction of the tire with changing temperature.

Pressure, speed and operating forces will affect tire temperature. High temperatures can be achieved with excessive camber, running with low inflation pressures (or a slow leak), or by using a tire made from a compound that is too soft for the track (such as using rain tires on a dry track) (Ref 2).

FRICTION CIRCLES AND G-G DIAGRAMS

There is much discussion about how many lateral g's a vehicle can withstand. What some may overlook is when the driver is at the maximum number of lateral g's and brakes or accelerates, the vehicle's tires may break away. Breaking or accelerating produces a longitudinal component of force that must be considered with the lateral force vector. Since the resultant force, or acceleration, is greater than either component alone, the introduction of either when driving at the vehicle's handling limits may cause tire break away. The resultant force, regardless of direction, is limited by the product of the vertical load and coefficient of friction. It is for this reason that friction circles (or ellipses) and "g-g" diagrams are constructed. These diagrams provide the user with information on the vehicles limitations (maximum force capability) over a range of possibilities. A friction circle or g-g diagram in vehicle handling is analogous to Mohr's Circle for structures. The friction circle and g-g diagram could be viewed as the practical way to use many of the tire characteristics discussed above.

The friction circle often plots slip ratios against lateral force while the g-g diagrams plot lateral acceleration vs. longitudinal acceleration, both for a given set of conditions. The friction circle is limited by the coefficient of friction where as the boundary of the g-g diagram depends on the speed of the vehicle. Some of these diagrams may show a theoretical boundary that is further outside the plot than the actual boundary (Figure 10 b). Vehicles cannot reach this boundary due to traction limitations, load transfer effects, suspension effects, limiting stability balance, and brake balance (Ref 4). Examples of g-g diagrams are shown in Figure 10.

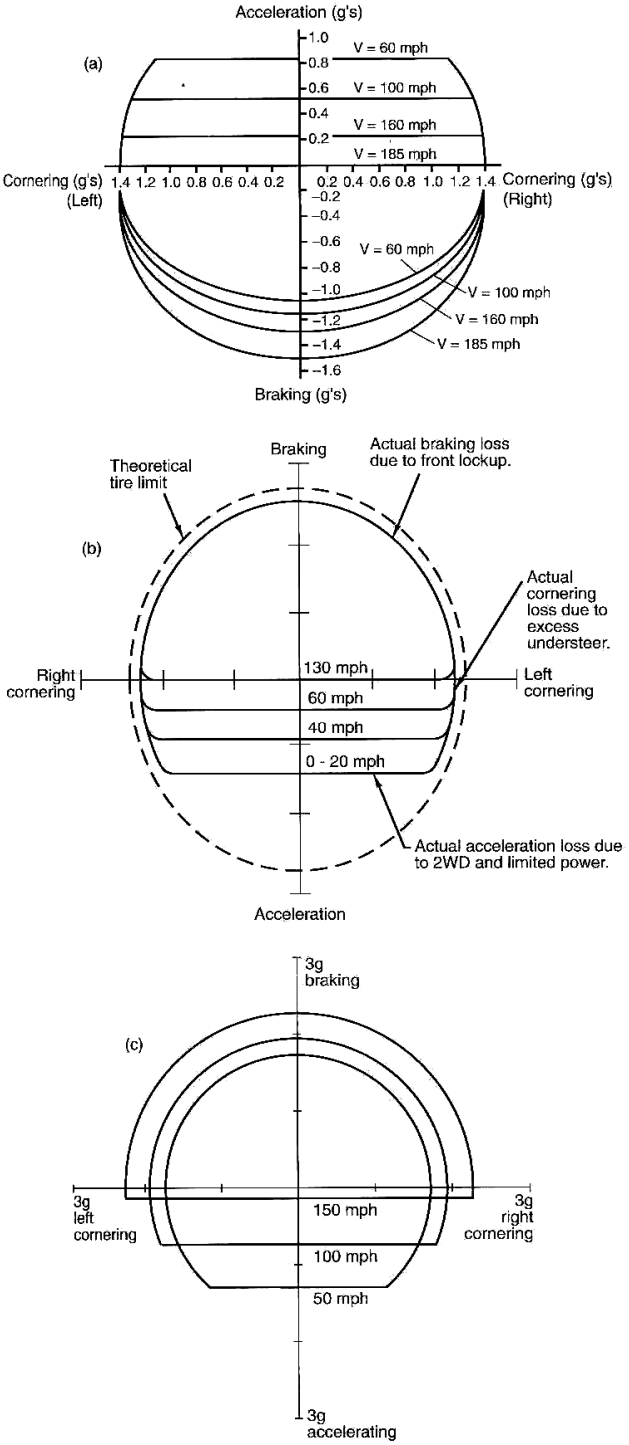

Figure 10 – Example G-G Diagrams (Ref 4)

Data can be taken to obtain actual g-g diagrams for individual vehicles at the tested conditions. This is done using accelerometers and data sampling instrumentation. Reference 4 should be consulted for more information on the application and use of g-g diagrams and where to obtain measurement equipment.

CONCLUSION

The tire is one of the most important components on a racecar. Knowledge of how the tire operates can give the engineer insight into design considerations and can yield information on the capabilities of a vehicle. Knowing these capabilities can be the difference between winning a race, or having tires break away through a turn and finishing last.

Thorough knowledge of how the above characteristics affect a vehicles capabilities and handling can be very useful. Specifically, the use of tire slip curves, either published from the manufacturer or determined by the user's testing, can be very useful. Knowledge of the principle forces involved in tire dynamics as well as weight transfer sensitivity, self-aligning torque and g-g diagrams can also be vitally useful tools for the engineer.

These characteristics are those deemed important by the design judges for formula SAE. It is the intent of the author that this short discussion of tire terminology will benefit future Colorado State FSAE students in two ways; it will allow them to quickly grasp the concepts and considerations dealing with tires, but it is also anticipated that the specific examples and numbers will give students a feel for what the values of the different parameters may be for a typical FSAE vehicle. While the capabilities were not available to the author at the time of composition, it would be a worthwhile task to model the Colorado State University FSAE tire in Adams/Tire® and compare the results with measured data. Modeling the tire either with simple formulas or with a computer program such as Adams could also become useful in tire selection if ample data is available.

REFERENCES

1. Dixon, J.C. (1996). Tires, Suspension and Handling 2nd ed. Warrendale: Society of Automotive Engineers.
2. Smith, C. (1978) Tune to Win. Fallbrook: Aero Publishers.
3. Gim, G, & Choi, Y. (Nov. 2001) Role of Tire Modeling on the Design Process of a Tire and Vehicle System. Hancook Tire Company Ltd.
4. Milliken, W.F., & Milliken, D.L. (1995) Race Car Vehicle Dynamics. Warrendale: Society of Automotive Engineers.
5. Lacombe, J. (2000) Tire Model for Simulations of Vehicle Motion on High and Low Friction Road Surfaces. U.S. Army Engineer Research and Development Center, Hanover, NH.
6. ASkelan, D, & Phule, P. (2003) The Science and Egineering of Materials. Pacific Grove: Brooks/Cole
7. Avallone, E, & Baumeister III, T. (1996). Marks' Standard Handbook For Mechanical Engineers 10th Edition. McGraw Hill
8. Skaggs, A. (2003) Suspension Loads and Spring Rate Analysis. Unpublished Technical Senior Design Contribution, Colorado State University.
9. Avon Tires, Downloads http://www.avonracing.com
10. Hoosier Tires, Colligate Formula SAE http://www.hoosiertire.com/rrtire.htm

CONTACT

Nicholas D. Smith smithn@engr.colostate.edu

RECCOMENDED READING

Tire Friction

1. The Unified Theory of Tire and Rubber Friction by H.W. Kummer and W.E. Mayer

2. The Physics of Tire Traction edited by D.F. Hays and A.L. Brooke

Various factors including horsepower loss from slip heating

3. Understanding Racing Tires by Chuck Hallum SAE Paper # 983028

DEFINITIONS, ACRONYMS, ABBREVIATIONS

γ - Camber Angle [deg]

μ - Coefficient of Friction [-]

α - Slip Angle [deg]

μ_R – Coefficient of Rolling Friction [-]

c – Foundation Stiffness [psi]

C_γ - Camber Stiffness [$^{lbf}/_{deg}$]

C_α - Cornering Stiffness [$^{lbf}/_{deg}$]

C_C – Camber Stiffness Coefficient [$^{1}/_{deg}$]

C_{FT} – Load Transfer Sensitivity [-]

C_{FV} – Ratio of Change in F_Y to F_V [-]

C_S – Cornering Stiffness Coefficient [$^{1}/_{deg}$]

C_Y – Lateral Force Coefficient [-]

CSU – Colorado State University

F_D – Tire Drag Force [lbf]

F_S – Tire Central Force [lbf]

F_V – Normal Force [lbf]

F_{VT} – Transferred Vertical Load [lbf]

F_X – Longitudinal Force [lbf]

F_Y – Lateral Force [lbf]

F_Z – Vertical Force [lbf]

FSAE – Formula SAE

K_{CSFV} – Sensitivity of C_S to F_V [-]

l – Tire footprint length [in]

M_Z – Self Aligning Torque (Moment) [lbf * ft]

t – Pneumatic Trail [in]

Ω_0 – Angular velocity of free rolling wheel [$^{rad}/_{s}$]

Ω - Angular velocity of driven wheel [$^{rad}/_{s}$]

$\dot{\Omega}$ - Angular velocity of wheel [$^{rad}/_{s^2}$]

V – Velocity [$^{ft}/_{s}$]

R_e – Effective radius of free rolling tire [ft]

R_l – Loaded Tire Radius [ft]

T – Thrust [lbf]

D – Drag [lbf]

F_R – Rolling Resistance [lbf]

T_{in} – Input torque to wheel [lbf * ft]

SAE – Society of Automotive Engineers.

APPENDIX

INFORMATION CONTAINED IN APPENDIX:

1. Avon Tire Data
2. Hoosier Tire Data
3. Example Calculations Using Given Avon Tire Data
4. Example Calculations Using A Few Selected Equations

AVON TIRE CURVES

Presented here is technical data given for Avon Tires (Ref 9). This tire is very similar to that used by many FSAE Teams. The CSU 2004 FSAE team will be using Hoosier tires with a 2° camber (available data is shown below in Table 1). While the tires are not the same, the following information should give the reader an estimate of what the lateral force and self-aligning moments could be.

Project:	**RC353STB**	**Size:**	**7.0/20.0-13**	**Camber:**	**2°**
Spec:	**10998**	**Tyre:**	**3 ply Pro Series**	**Pressure:**	**26 P.S.I.**
Tested:	**31/07/01**	**Rim:**	**6 x 13**	**Speed:**	**20 KPH**

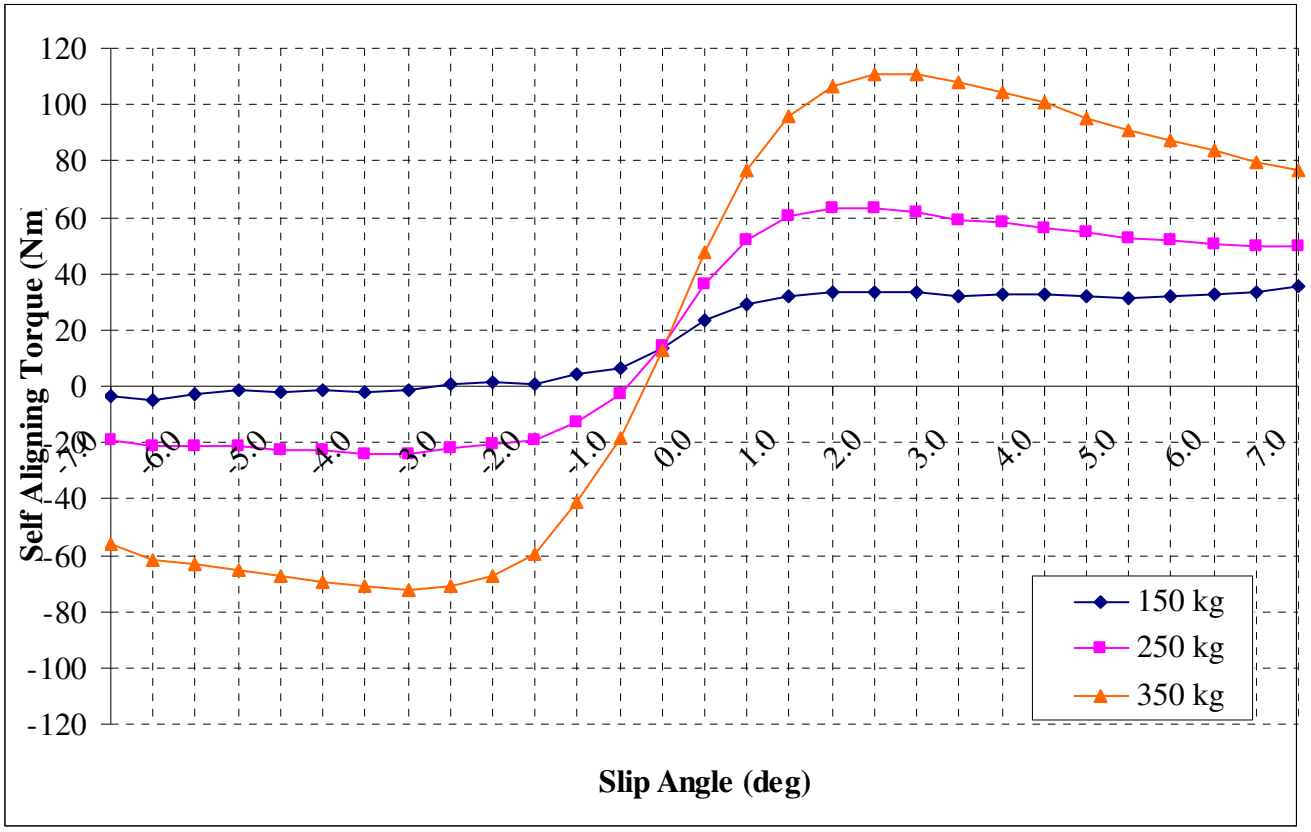

Figure 11 - Self-Aligning Torque vs. Slip Angle (Ref 9)

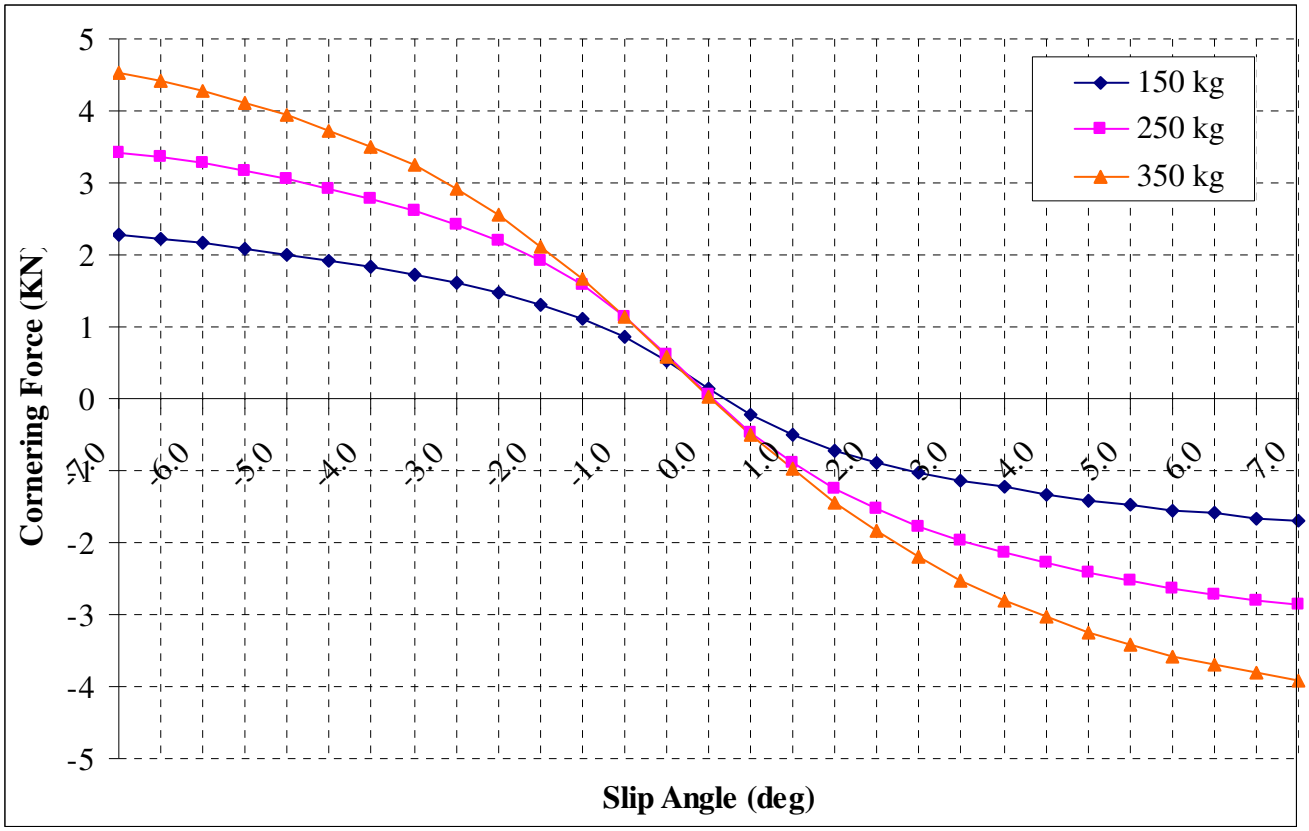

Figure 12 - Cornering Force vs. Slip Angle (Ref 9)

Project:	**RC353STB**		**Size:**	**7.0/20.0-13**		**Camber:**	**1°**
Spec:	**10998**		**Tyre:**	**3 ply Pro Series**		**Pressure:**	**26 P.S.I.**
Tested:	**31/07/01**		**Rim:**	**6 x 13**		**Speed:**	**20 KPH**

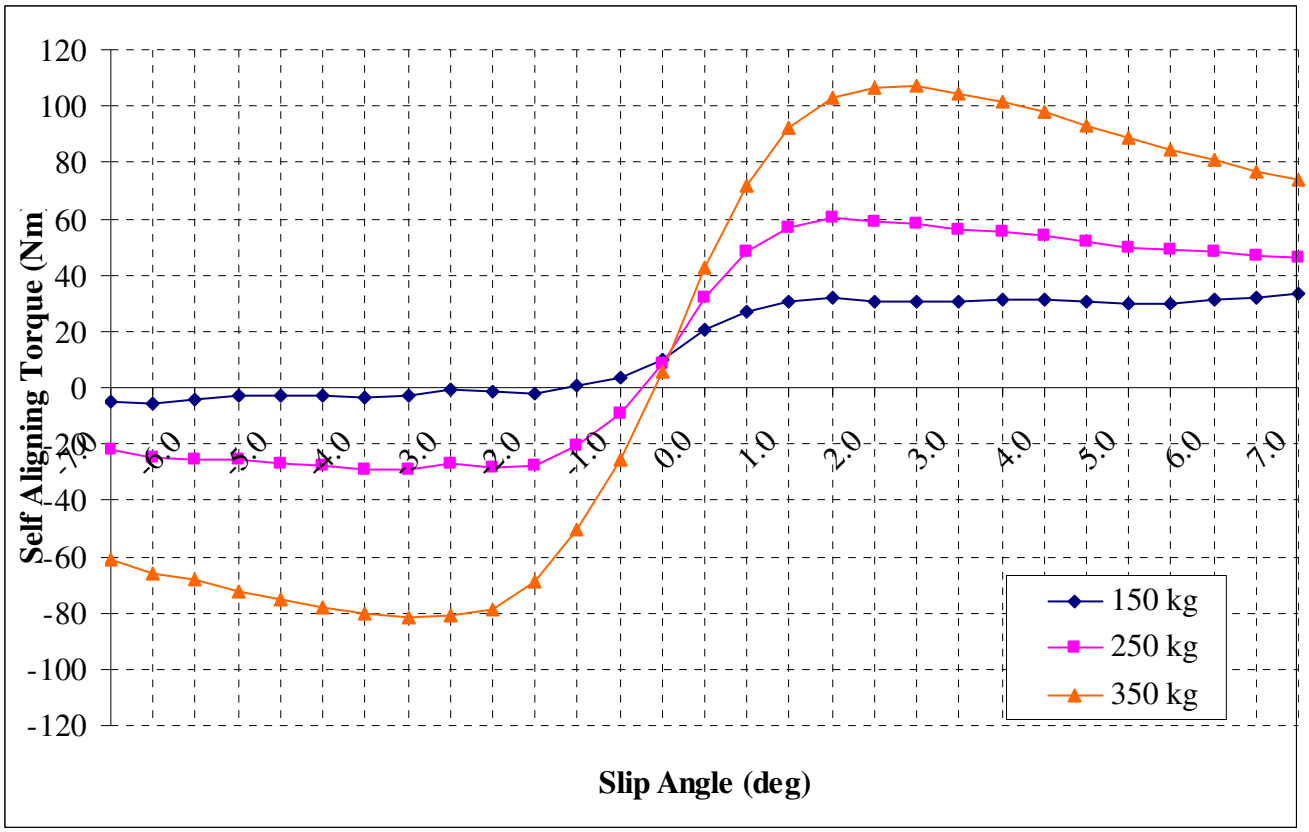

Figure 13 - Self-Aligning Torque vs. Slip Angle (Ref 9)

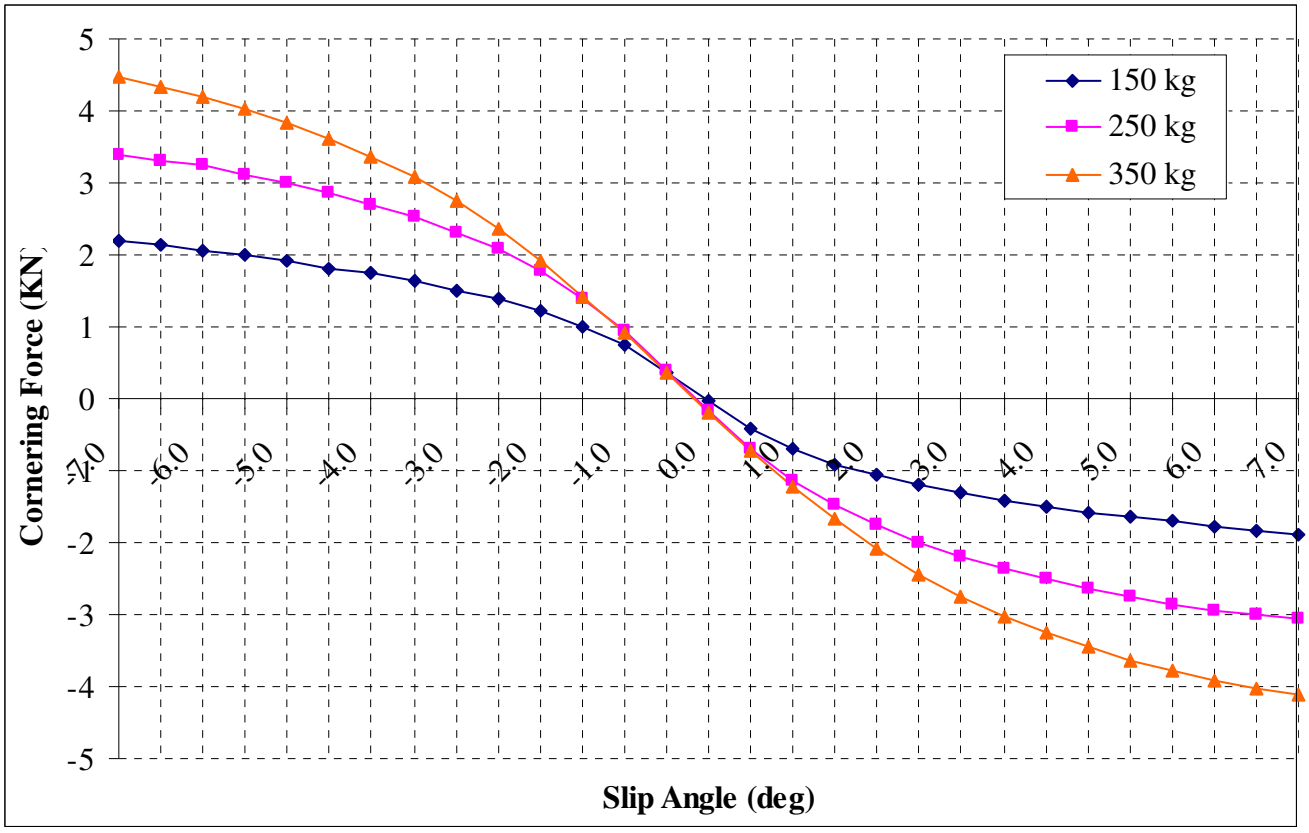

Figure 14 - Cornering Force vs. Slip Angle (Ref 9)

Lateral Force vs Slip Angle At 1deg Camber and 330 lbf (150kg) Normal Load

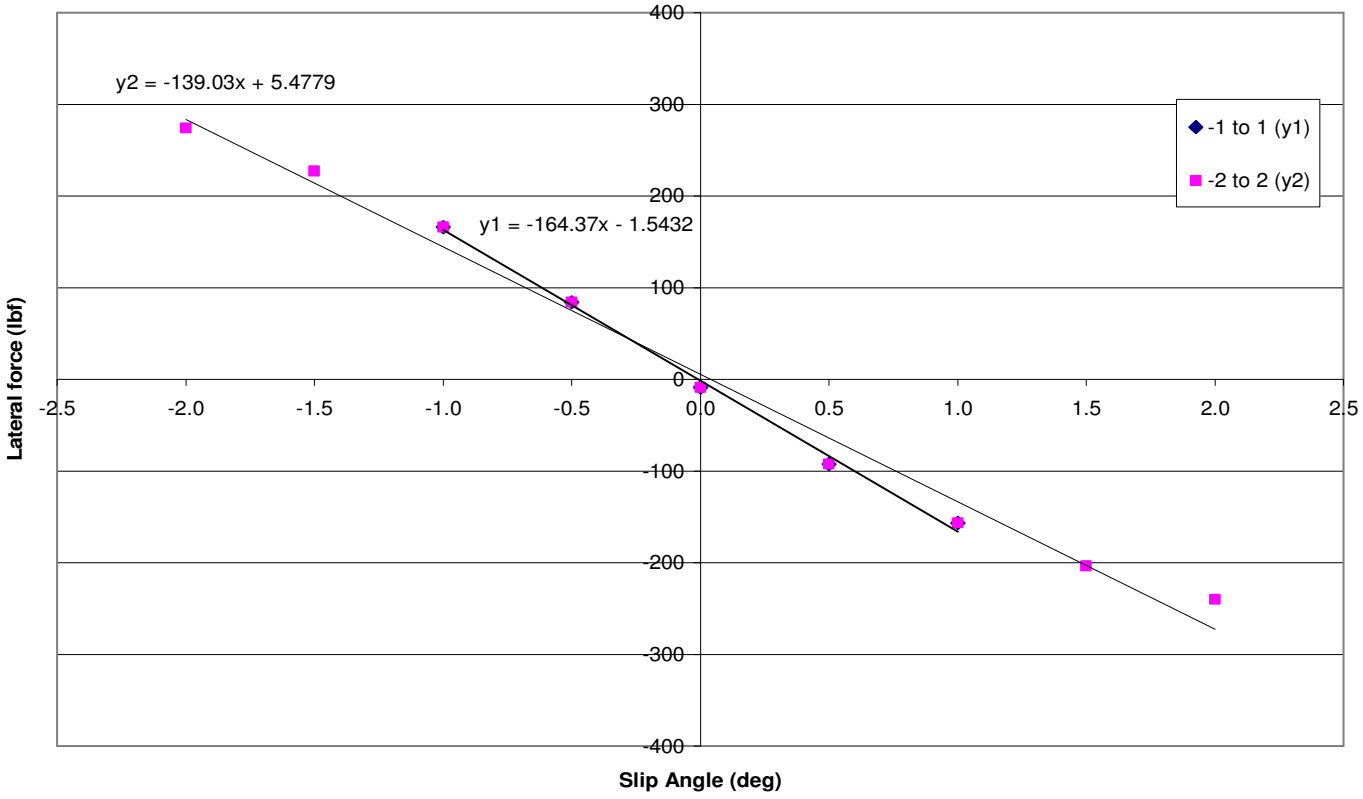

Figure 15 - Lateral Force vs. Slip Angle for Different Ranges of Slip Angle (Data taken from Ref 9)

HOOSIER TIRE DATA

TIRE SIZE: 20.0 x 7.0 - 13 COMPOUND = R25A RIM WIDTH = 8" PRELOAD = 0			
AIR = 18 PSI	**DEFLECTION** (in)	**ACTUAL LOAD** (lbs)	**SPRING RATE** (lbs/in)
	0.2	144	720
	0.4	314	785
	0.6	490	816.67
	0.8	655	818.75
	1	821	821
AIR = 16 PSI	**DEFLECTION** (in)	**ACTUAL LOAD** (lbs)	**SPRING RATE** (lbs/in)
	0.2	123	615
	0.4	288	720
	0.6	451	751.67
	0.8	618	772.5
	1	783	783
AIR = 14 PSI	**DEFLECTION** (in)	**ACTUAL LOAD** (lbs)	**SPRING RATE** (lbs/in)
	0.2	123	615.00
	0.4	275	687.50
	0.6	430	716.67
	0.8	582	727.50
	1	749	749.00

Table 1 – Hoosier Tire Data (Ref 10)

Example Calculations for the Avon Tire

Point of interest: **Slip angle:** $\alpha := 1.3 \cdot deg$

Camber Angle: $\gamma := 1 \cdot deg$

Load on Tire $F_V := 150 \cdot kg \cdot g$ $F_V = 330.693 lbf$

Coefficient of Friction $\mu := 1.5$

Known Lateral Load and Moments:

Slip angle: $\alpha_1 := 1.5 \cdot deg$ **Lateral Force:** $F_{Y1} := 203.64 lbf$

$\alpha_2 := 1 \cdot deg$ $F_{Y2} := 156.59 lbf$

$\alpha_3 := 0.5 \cdot deg$ $F_{Y3} := 92.3 \cdot lbf$

Self Aligning Torque:

$M_{Z1} := 23.32 lbf \cdot ft$

$M_{Z2} := 22.516 lbf \cdot ft$

$M_{Z3} := 19.76 lbf \cdot ft$

Quadratic Spline Interpolation:

$$F_Y(\alpha) := \frac{(\alpha - \alpha_2)\cdot(\alpha - \alpha_3)}{(\alpha_1 - \alpha_2)\cdot(\alpha_1 - \alpha_3)} \cdot F_{Y1} + \frac{(\alpha - \alpha_1)\cdot(\alpha - \alpha_3)}{(\alpha_2 - \alpha_1)\cdot(\alpha_2 - \alpha_3)} \cdot F_{Y2} + \frac{(\alpha - \alpha_1)\cdot(\alpha - \alpha_2)}{(\alpha_3 - \alpha_1)\cdot(\alpha_3 - \alpha_2)} \cdot F_{Y3}$$

$$M_Z(\alpha) := \frac{(\alpha - \alpha_2)\cdot(\alpha - \alpha_3)}{(\alpha_1 - \alpha_2)\cdot(\alpha_1 - \alpha_3)} \cdot M_{Z1} + \frac{(\alpha - \alpha_1)\cdot(\alpha - \alpha_3)}{(\alpha_2 - \alpha_1)\cdot(\alpha_2 - \alpha_3)} \cdot M_{Z2} + \frac{(\alpha - \alpha_1)\cdot(\alpha - \alpha_2)}{(\alpha_3 - \alpha_1)\cdot(\alpha_3 - \alpha_2)} \cdot M_{Z3}$$

Lateral Force: $F_Y(1.3 \cdot deg) = 186.889 lbf$ $F_Y(1.3 \cdot deg) = 831.323 N$

Self Aligning Torque: $M_Z(1.3 \cdot deg) = 23.233 lbf \cdot ft$ $M_Z(1.3 \cdot deg) = 31.499 N \cdot m$

Pneumatic Trail $t := \frac{M_Z(1.3 \cdot deg)}{F_Y(1.3 \cdot deg)}$ $t = 1.492 in$ $t = 37.89 mm$

Contact Patch Length $l := 6 \cdot t$ $l = 8.951 in$ $l = 227.343 mm$

Approximate Cornering Stiffness $C_\alpha := \frac{F_Y(1.3 \cdot deg)}{1.3 \cdot deg}$ $C_\alpha = 143.761 \frac{lbf}{deg}$ $C_\alpha = 639.479 \frac{N}{deg}$

Normal Load Sensitivity:

Tire Data: $\alpha_1 := 1.5 \cdot deg$ $F_{Y1} := 203.64 lbf$ $F_{V1} := 150 \cdot kg \cdot g$ $F_{V1} = 330.693 lbf$

$\alpha_2 := 1.5 \cdot deg$ $F_{Y2} := 332 \cdot lbf$ $F_{V2} := 250 \cdot kg \cdot g$ $F_{V2} = 551.156 lbf$

$$C_{FV} := \frac{F_{Y2} - F_{Y1}}{F_{V2} - F_{V1}} \qquad C_{FV} = 0.582$$

Lateral Force From Slip angle

Vertical Load: $F_V := \frac{800 \cdot lbf}{4}$ $F_V = 200lbf$ $F_V = 889.644N$

Coefficient of Friction $\mu := 1.5$

Foundation Stiffness $c := 5 \cdot 10^6 \cdot Pa$ $c = 725.189psi$

Contact Patch Length $l := 8.5 \cdot in$ $l = 215.9mm$

Lateral Force: $F_Y(\alpha) := \mu \cdot F_V - \frac{\mu^2 \cdot F_V^2}{2 \cdot c \cdot l^2 \cdot \tan(\alpha)}$

Slip Angle Range: $\alpha := 0, 0.001 .. 20 \cdot deg$

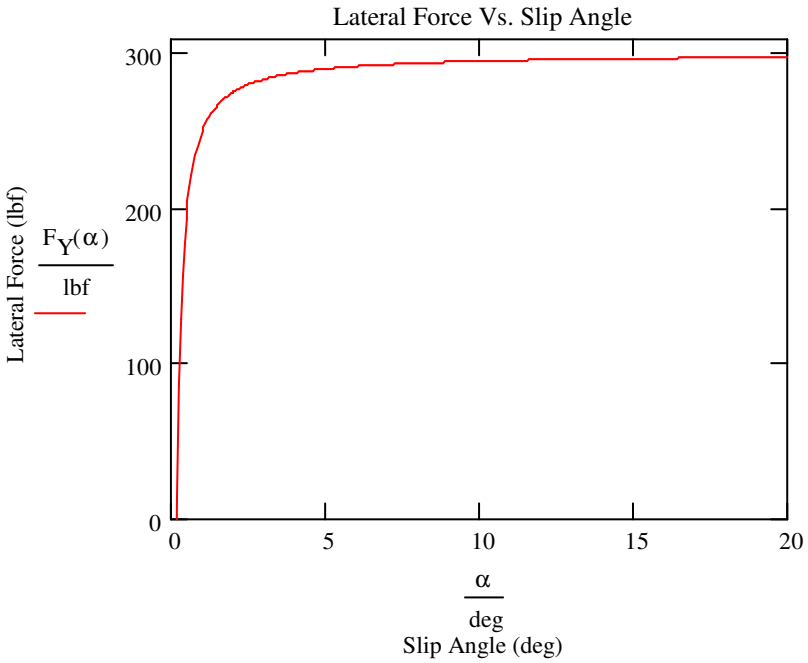

$\frac{F_Y(3 \cdot deg)}{F_Y(90 \cdot deg)} = 0.945$

Camber Angle

Camber Stiffness Coefficient $C_C := \frac{0.018}{deg}$

Normal Load Range $F_V := 50, 50.1 .. 500$

Lateral Force $F_Y(\gamma, F_V) := C_C \cdot F_V \cdot \gamma$

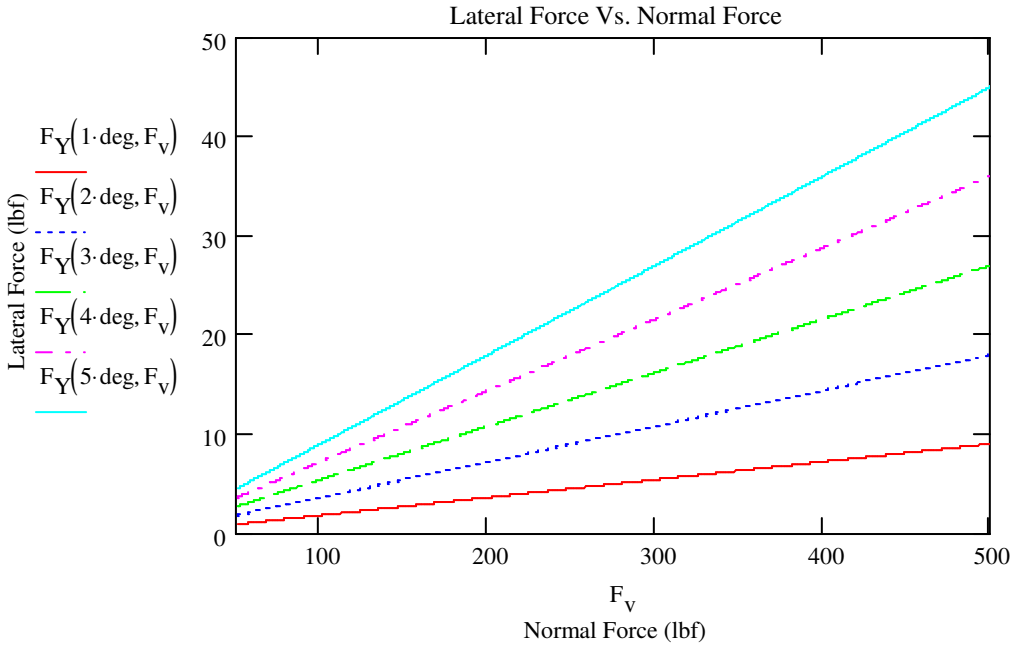

Self Aligning Torque

$$M_Z(\alpha, F_V) := \frac{\mu^2 \cdot F_V^2}{4 \cdot c \cdot l \cdot \tan(\alpha)} - \frac{\mu^3 \cdot F_V^3}{6 \cdot c^2 \cdot l^3 \cdot (\tan(\alpha))^2} \qquad \alpha := 0, 0.001 .. \frac{\pi}{2}$$

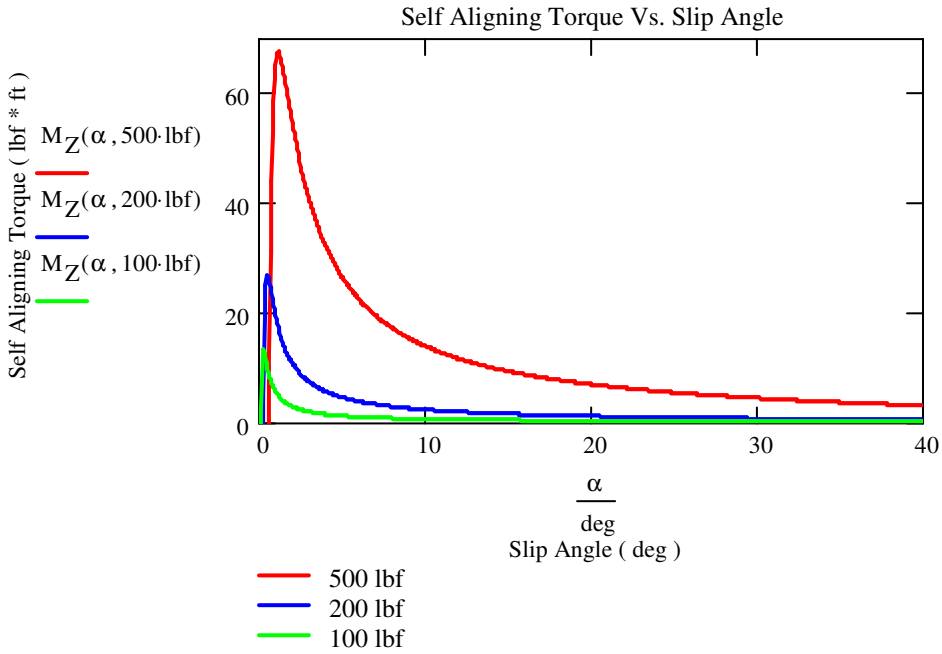

Pneumatic Trail

Normal Load $F_V := 200\,lbf$

$$F_Y(\alpha) := \mu \cdot F_V - \frac{\mu^2 \cdot F_V^2}{2 \cdot c \cdot l^2 \cdot \tan(\alpha)}$$

Pneumatic Trail (Equation 21)

$$t(\alpha) := \frac{M_Z(\alpha, F_V)}{F_Y(\alpha)}$$

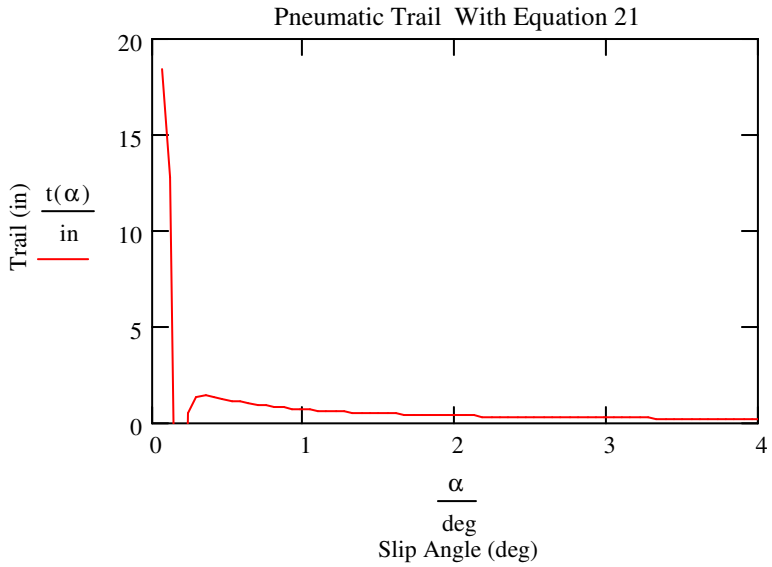

Pneumatic Trail (Equation 22)

$$t(\alpha) := \frac{3 \cdot \mu \cdot F_V \cdot c \cdot l^2 \cdot \tan(\alpha) - 2 \cdot \mu^2 \cdot F_V^2}{12 \cdot c^2 \cdot l^3 \cdot (\tan(\alpha))^2 - 6 \cdot \mu \cdot F_V \cdot c \cdot l \cdot \tan(\alpha)}$$

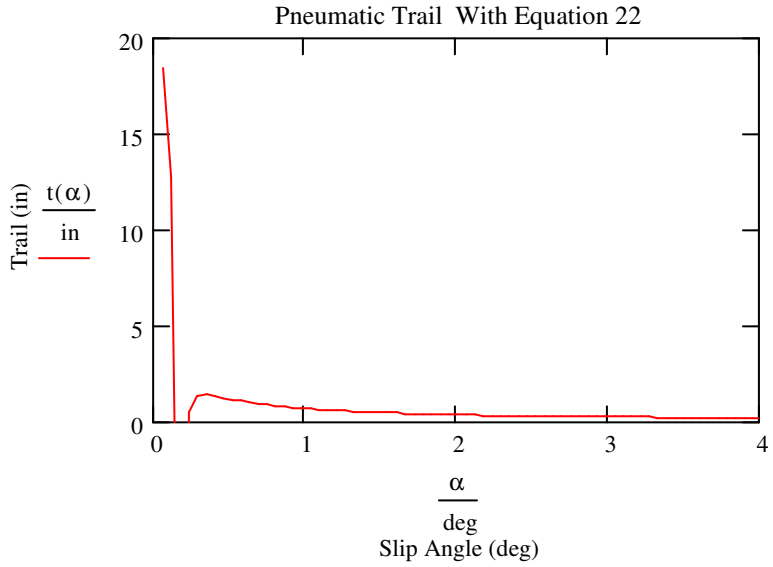

Load Transfer Sensitivity

$$C_S := \frac{0.14}{deg}$$

$$F_Y(\alpha, F_v) := C_S \cdot F_v \cdot \alpha$$

$$F_v := 50, 50.1 .. 500$$